Supplementary Information for the manuscript

Calcium signalling mediates self-incompatibility response in the Brassicaceae

Megumi Iwano, Kanae Ito, Sota Fujii, Mitsuru Kakita, Hiroko Asano-Shimosato, Motoko Igarashi, Pulla Kaothien-Nakayama, Tetsuyuki Entani, Asaka Kanatani, Masashi Takehisa, Masaki Tanaka, Kunihiko Komatsu, Hiroshi Shiba, Takeharu Nagai, Atsushi Miyawaki, Akira Isogai & Seiji Takayama*

*Corresponding author, E-mail: takayama@bs.naist.jp

This supplementary pdf file contains the following information

Other Supplementary Materials for this manuscript includes the following:

Supplementary Methods

Generation of transgenic plants and the vector construction processes.

All transgenic plants were generated in *A. thaliana* accession C24 using the *Agrobacterium* infiltration procedure, as previously reported[28]. We chose C24 as the host accession, because this strain was already shown by the others that SI expression is feasible[23]. Self-incompatible transgenic plants of *A. thaliana* C24 were produced by introducing S_b-*SP11/SCR* and S_b-*SRK* genes derived from the S_b-haplotype of self-incompatible *A. lyrata*. For S_b-*SP11/SCR* expression in anther, the S_b-SP11$_{pro}$:GW/pBI121 binary vector was generated by substitution of 35S promoter of pBI121 (Clontech) with the 522-bp promoter region of S_9-*SP11/SCR*[50] and GUS gene of pBI121 for Gateway cassette. The coding region of S_b-*SP11/SCR* was re-amplified from its synthetic gene (Gene Design Inc., Osaka, Japan) by PCR using primers, 5'-ATGAGGAATGCTACTTTCTTC-3' and 5'-TAGCAAAATCTACAGTCGCATA-3' and cloned into pCR8/GW/TOPO vector (Invitrogen). S_b-*SP11/SCR* was transferred to S_9-SP11$_{pro}$:GW /pBI121 vector. For S_b-*SRK* expression in papilla, *ΨSRK* promoter was amplified from *A. thaliana* (Col-0) genomic DNA by PCR using primers 5'-AAGCTTAATTTCGGGTTGTACGTTTTGAGA-3' and 5'-GAGCTCAAGGTACCATGTTGTTCATTTTCC-3' (underlined sequence indicating the incorporated *Hind*III and *Kpn*I site) and cloned into pBI121 or pRI909 (TaKaRa) by enzymatic digestion with *Hind*III and *Kpn*I. ΨSRK$_{pro}$:GW/pBI121 and ΨSRK$_{pro}$:GW/pRI909 were obtained by insertion of Gateway cassette into pBI121 and pRI909 *Kpn*I blunting site. S_b-*SRK* was amplified from *A. lyrata* (S_b) stigmatic cDNAs by PCR using primers SRKb_F: 5'-ATGAGAGTTGTAGTACCAAACTGC-3' and SRKb_R: 5'-TTACCGAGGGTCGATGGC-3'. The amplified S_b-*SRK* fragment was cloned into pCR8/GW/TOPO and then transferred to the ΨSRK$_{pro}$:GW/pBI121. For kinase-inactive S_b-SRK_K555E expression, the S_b-*SRK _K555E* cDNA fragment was generated by 2 steps PCR. The 1st PCR were performed individually using two primer pairs SRKb_F and 5'-GAGATTGCGGTGAGAAGGCTA-3', and SRKb_R and 5'-TAGCCTTCTCACCGCAATCTC-3' and generated two overlapping S_b-*SRK* fragments. The full length of S_b-*SRK_K555E* was reconstituted by the 2nd PCR from

two 1st PCR fragments using SRKb_F and SRKb_R primers. This fragment was cloned into pCR8/GW/TOPO and transferred to ΨSRK_{pro}:GW/p909.

For expressing YC3.60 and YC3.60$_{pm}$ in papilla cells, the vectors SRK9$_{pro}$:YC3.60 and SRK9$_{pro}$:YC3.60$_{pm}$ were constructed as follows: a DNA fragment encoding YC3.60 was obtained by digestion of plasmid pcDNA-YC3.60 with *Eco*RI and *Hind*III, and blunted; pBI121 (Clontech) was digested with *Bam*HI and *Sac*I, and blunted; and the YC3.60 fragment was ligated into the pBI121 backbone to yield pBIYC3.60. The *B. rapa* S_9*-SRK* promoter sequence, used for papilla cell–specific expression, was amplified by PCR using primers that incorporated *Sph*I and *Sma*I sites into its 5'- and 3'-termini, respectively: forward primer, 5'-GCATGCAAAGCATGCATTGAATTATTAGA-3'; reverse primer, 5'-CCCGGGCTCTCTCCCCACCTTTTTCTTTC-3'. For those PCRs, the P1-derived artificial chromosome clone E89, containing the S_9*-SRK* flanking sequence[51], was used as a template. The amplified DNA fragment was digested with *Sph*I and *Sma*I and ligated into pBIYC3.60 (digested with *Sph*I and *Not*I, and then blunted) to yield pBI-SRK9$_{pro}$:YC3.60. SRK9$_{pro}$:YC3.60 digested with *Hind*III was ligated into the *Hind*III site of pSLJ1006 (ref. 52) to yield pSRK9YC3.60. A *YC3.60$_{pm}$*-encoding fragment was obtained by digestion of plasmid pcDNA-YC3.60$_{pm}$ with *Eco*RI and *Hind*III, and then cloned into the *Eco*RI and *Hind*III sites of pRI909 (Takara Bio) to yield pRI909-YC3.60$_{pm}$. The *nos* terminator (NosT) sequence of pBIYC3.60 was excised by digestion with *Eco*RI and ligated into the *Eco*RI site of pRI909-YC3.60$_{pm}$ to yield pRI909-YC3.6pm-NosT. SRK9$_{pro}$:YC3.6 was digested with *Hind*III and *Eco*52I, and the resultant S_9*-SRK* promoter fragment was cloned into the *Hind*III and *Not*I (cohesive with *Eco*52I) sites to yield SRK9$_{pro}$:YC3.60$_{pm}$. YC3.60$_{pm}$ localizes to plasma membrane via the CAAX box of Ki-Ras protein fused to the C-terminus of YC3.60 (ref. 27).

For the *GLR3.7* complementation experiment, at first *GLR3.7* promoter was PCR amplified using the primers GLR3.7p+ATG-F (5'-CTGTCGATATCAAAGTGCTGGATTCTCCT-3') and GLR3.7_cloning-R (5'-AATGCCCAGTCCCATGGAGATAATGCAATC-3'). *GLR3.7* cDNA was amplified by PCR using the primers GLR3.7p+ATG-F (5'-GATTGCATTATCTCCATGGGACTGGGCATT-3') and GLR3.7_cloning-R

(5'-TCAATTTCGTGGTACCTCAGTATC-3'). These two fragments were purified and fused by the second PCR using the primers GLR3.7p-F and GLR3.7_cloning-R. This fragment was cloned into pCR8/GW/TOPO (Life Technologies), sequenced and subcloned into the pCambia vector.

Selection of the transgenic lines used in this study. We first generated two lines, one expressing solely *S_b-SRK*, and another expressing *S_b-SP11/SCR*. For each construct harboring each gene, we selected the transformat seeds on an agar plate including kanamycin. Survived T_1 transformats of each line were pollinated with each other by using *S_b-SRK* introduced plants as the female parents and *S_b-SP11/SCR* introduced plants as the male parents, to further select the lines that exhibit SI phenotype. Selfed seeds from the selected lines (T_2 generation) were plated on an agar plate including kanamycin, to find the lines carrying the transgene on single chromosomal location. For each construct, lines that carry the transgene homozygously were obtained as the T_3 generation seeds. These lines were re-evaluated for their stableness in the SI phenotype by the pollination test, and one line for each construct was selected for use in the subsequent experiments. We also obtained a line that carries both *S_b-SRK* and *S_b-SP11/SCR* homozygously by genetic crosses (*S_b-SP11/SCR* expressing plant as female, *S_b-SRK* expressing plant as male). This line carrying both genes was confirmed to produce much less seeds (~100 seeds per individual) compared to the wild-type C24 accession, certifying the function of the introduced *S_b-SRK* and *S_b-SP11/SCR*.

In parallel, we obtained the lines expressing YC3.60 or $YC3.60_{pm}$ in the papilla cells by similar procedures. For each construct, a line strongly expressing the YC3.60 forms in the papilla cells, and carrying the transgene on single locus was selected. These lines were crossed with the established *S_b-SRK* expressing line described above, to obtain the lines co-expressing *YC3.60* forms and *S_b-SRK* at the same time. Single F_3 lines that carry both *S_b-SRK* and the *YC3.60* forms homozygously were selected for the subsequent experiments. In summary, all of the *S_b-SRK* expressing lines used in this study are the progenies of a single line, and thus transgenic variations do not have to be taken into consideration in this study.

Screening of the TILLING lines of the *GLR* genes. We used the TILLING platform for screening C24 genetic background mutants previously developed[53]. Using this platform, we obtained nonsense mutants for each of the four *GLR* genes. For each *glr1.3, glr3.3, grl3.5* and *glr3.7* mutants, 491th tryptophan, 252th tryptophan, 462th tryptophan and 765th tryptophan was altered into a stop codon (Supplementary Figure 12). These lines in M_3 generation were crossed with the S_b-*SRK/YC3.60* co-expressing line, and progenies carrying the *glr* mutations, and S_b-*SRK* and *YC3.60* were selected in the F_2 generation to investigate the effect of these mutations on the Ca^{2+}-dynamics upon SI response. Progenies that lost the *glr* mutations were also obtained through this selection process, and used as the control for the protoplast assay.

Complementation of the *glr3.7* mutation by *GLR3.7*$_{pro}$:*GLR3.7* cDNA construct. The *GLR3.7*$_{pro}$:*GLR3.7* cDNA construct was introduced into the *glr3.7* nonsense mutant homozygously carrying S_b-*SRK* and *YC3.6*. T_1 transformats were selected on an agar plate containing hygromycin.

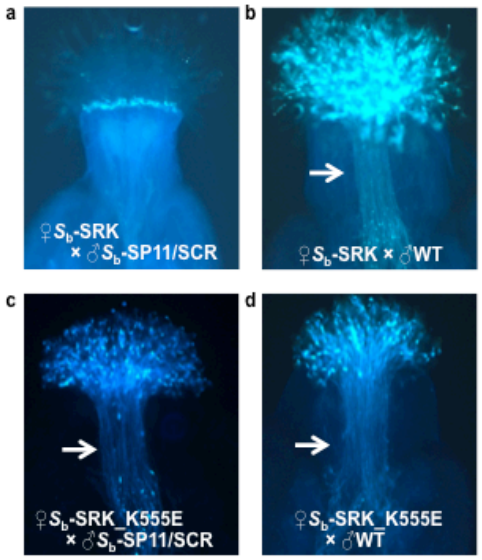

Supplementary Figure 1 | SI phenotype of *A. thaliana* C24 transformant expressing S_b-SP11/SCR and S_b-SRK. (**a**) S_b-SRK–expressing stigma was pollinated with self (S_b-SP11/SCR–expressing) pollen grains. (**b**) S_b-SRK–expressing stigma was pollinated with cross (WT) pollen grains. (**c**) Kinase-inactive S_b-SRK_K555E–expressing stigma was pollinated with S_b-SP11/SCR–expressing pollen grains. (**d**) S_b-SRK_K555E–expressing stigma was pollinated with WT pollen grains. Compatible and incompatible pollinations were judged by monitoring the pollen tube growth after aniline blue staining. Arrows indicate the pollen tube growth.

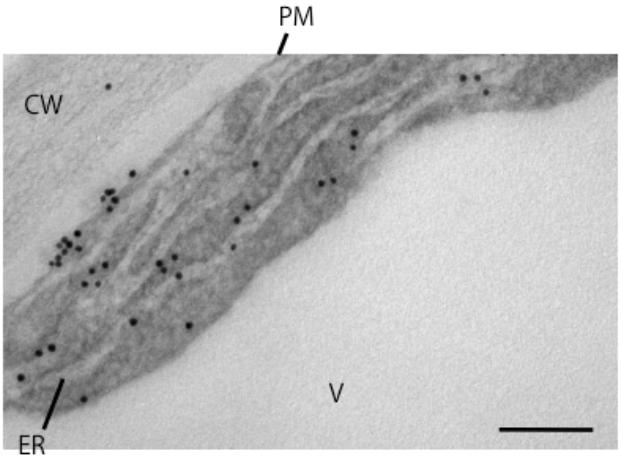

Supplementary Figure 2 | Localization of YC3.60$_{pm}$ in the stigmatic papilla cell. YC3.60 signals were observed on the cytoplasmic faces of the plasma membrane and ER membrane. For detection of YC3.60, anti-GFP mouse antibody (primary antibody), and 10-nm gold particle–conjugated anti–mouse IgG antibody (secondary antibody) were used. CW, cell wall; PM, plasma membrane; ER, endoplasmic reticulum; V, vacuole. Bar, 0.2 μm.

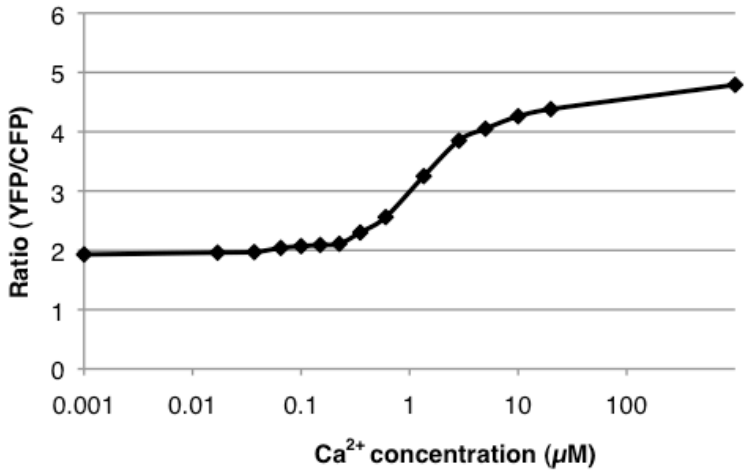

Supplementary Figure 3 | Titration curve for YC3.60. Serial dilutions of purified YC3.60 were made in Ca^{2+} calibration buffer (Molecular Probes), in which the free [Ca^{2+}] ranged from 0–1 mM.

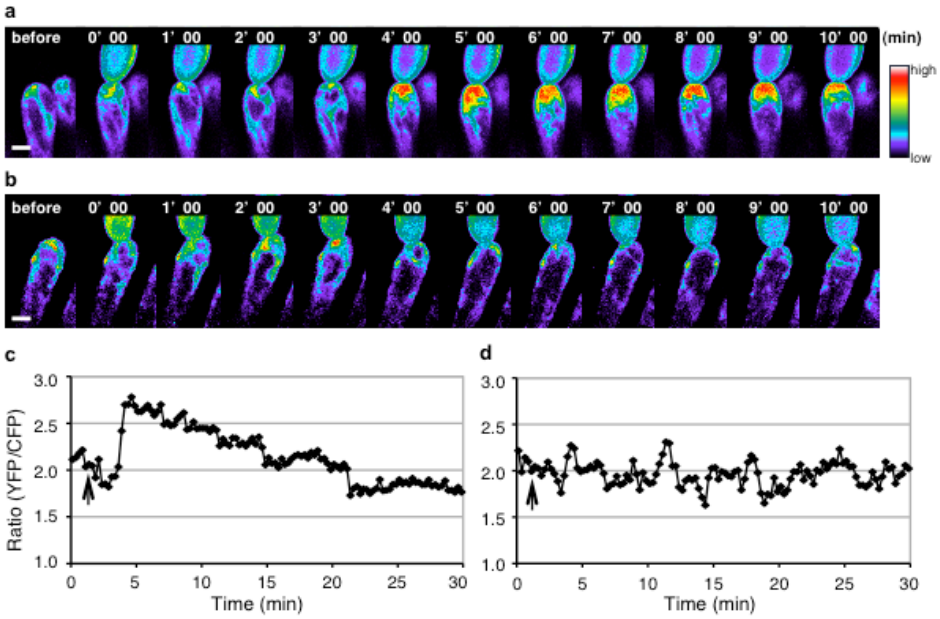

Supplementary Figure 4 | Dynamics of $[Ca^{2+}]_{cyt}$ in YC3.60 (soluble form)–expressing papilla cells following self- and cross-pollination. (**a**) YFP/CFP ratio images of a single S_b-SRK–expressing papilla cell before and after pollination with a self (S_b-SP11/SCR–expressing) pollen grain. (**b**) YFP/CFP ratio images of a single S_b-SRK–expressing papilla cell before and after pollination with a cross (WT) pollen grain. Scale bars, 5 μm. (**c**) The time-course ratio change in the tip region below the pollen attachment site after the self-pollination shown in (a). Before pollination the mean ratio was 1.99 ± 0.50 (n = 40), while it increases and reaches a maximum at ca. 5 min after self-pollination (the mean value of the time = 4.88 ± 1.9 min; the mean value of the maximum ratio = 2.55 ± 0.65, n = 20) (**d**) The time-course ratio change in the tip region below the pollen attachment site after the cross pollination shown in (b). No significant $[Ca^{2+}]_{cyt}$ change was observed (the ratio at 5 min after pollination was 2.01 ± 0.29, n = 20). Arrows indicate pollination timing.

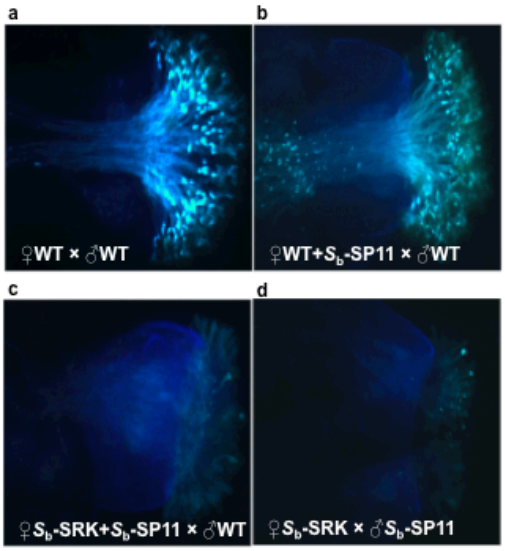

Supplementary Figure 5 | Biological activity of synthesized S_b-SP11/SCR as a male *S*-determinant. (**a**) WT *A. thaliana* accession C24 is self-compatible, and accept WT pollen grains. (**b**) When the synthesised S_b-SP11/SCR was applied to the WT stigma, WT pollen grains were also accepted. (**c**) When the synthesised S_b-SP11/SCR was applied to a S_b-SRK–expressing stigma, germination of WT pollen grains was arrested, as in the pollination of self (S_b-SP11/SCR–expressing) pollen grains (**d**).

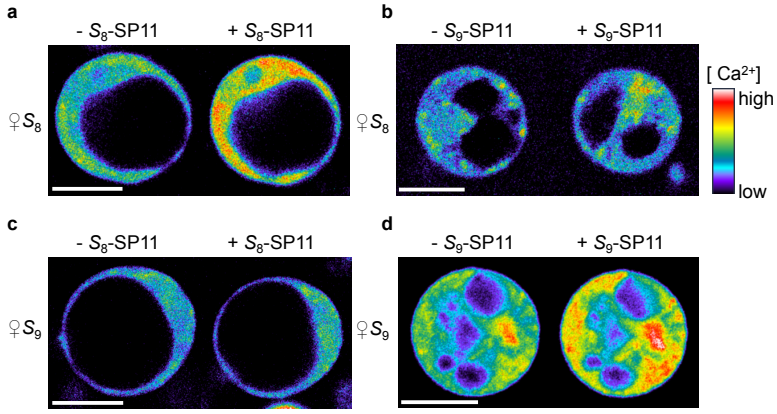

Supplemental Figure 6 | Effects of SP11/SCR on $[Ca^{2+}]_{cyt}$ dynamics in papilla-cell protoplasts from *B. rapa*. (a–d) Typical fluorescent images of Fluo4-AM-loaded papilla-cell protoplasts from *B. rapa* before (left) and after (right) the addition of SP11/SCR ligand (to 10 nM). Scale bars, 20 μm. **(a)** Papilla-cell protoplast from S_8-homozygote was treated with "self" S_8-SP11/SCR. **(b)** Papilla-cell protoplast from S_8-homozygote was treated with "cross" S_9-SP11/SCR. **(c)** Papilla-cell protoplast from S_9-homozygote was treated with "cross" S_8-SP11/SCR. **(d)** Papilla-cell protoplast from S_9-homozygote was treated with "self" S_9-SP11/SCR.

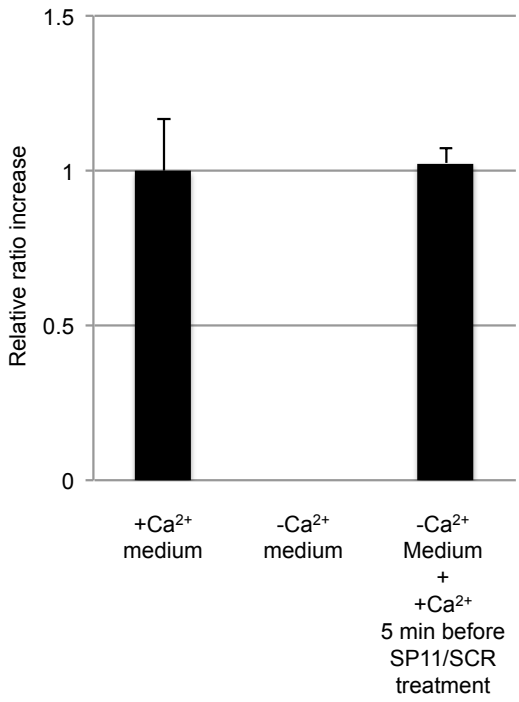

Supplemental Figure 7 | Restoration $[Ca^{2+}]_{cyt}$ increase ability during the SI response by Ca^{2+} addition. Protoplasts were once incubated in Ca^{2+}-free medium, and then 3 mM $CaCl_2$ at final concentration was added 5 min before SP11/SCR treatment. Relative YFP/CFP ratio increase after SP11/SCR treatment is indicated. Error bars indicate standard deviations (n = 3).

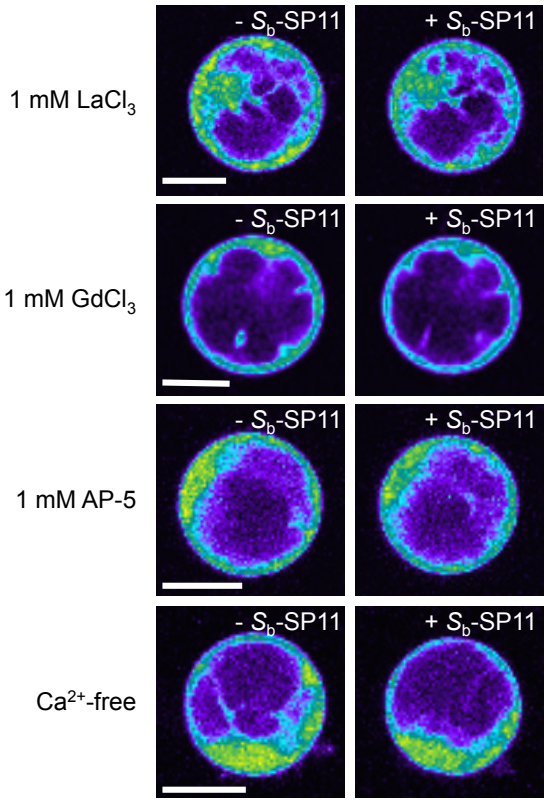

Supplementary Figure 8 | $[Ca^{2+}]_{cyt}$ dynamics in papilla-cell protoplasts in the SI response under different conditions when influx was severely affected. Typical ratio (YFP/CFP) images of YC3.60–expressing papilla-cell protoplasts before (left) and 6 min after (right) the addition of SP11/SCR ligand (to 10 nM).

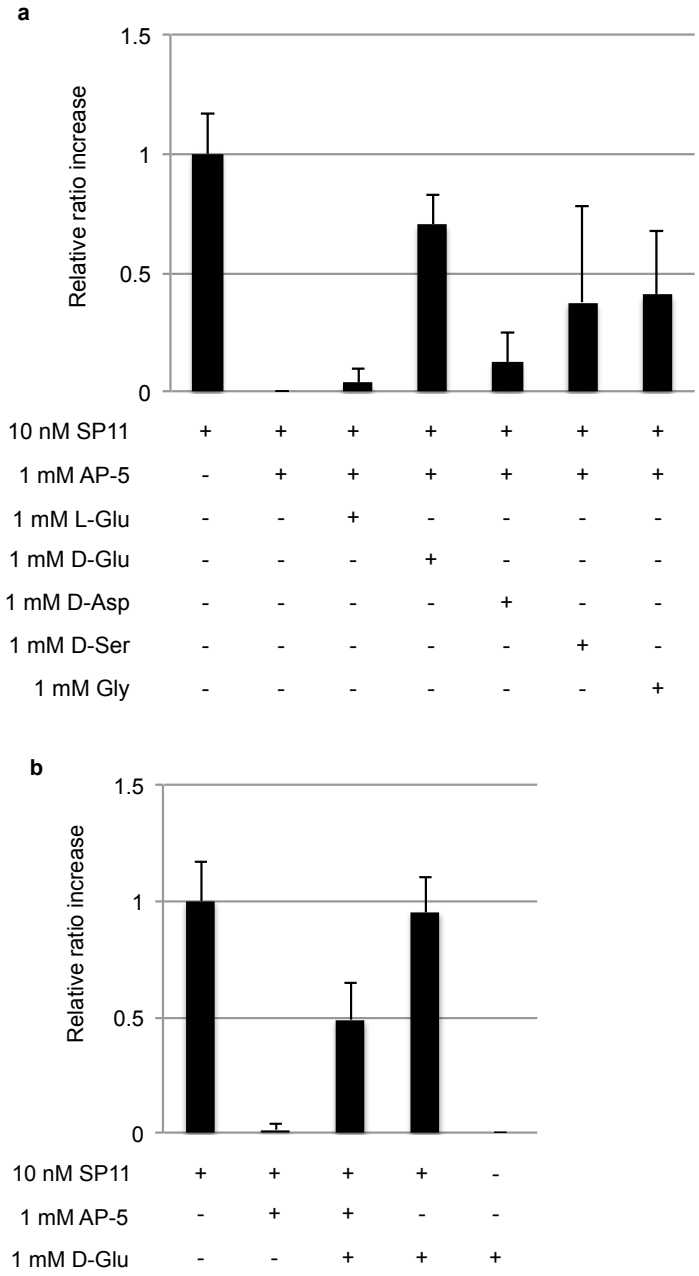

Supplementary Figure 9 | Putative GLR ligands compete with AP-5 to restore SP11/SCR-induced $[Ca^{2+}]_{cyt}$ increase response. (a) AP-5 or amino acids were treated to papilla cell protoplasts 15 min before SP11/SCR treatment. **(b)** SP11, AP-5 or D-Glu were simultaneously treated. Relative YFP/CFP ratio increase after SP11/SCR treatment is indicated. Error bars indicate standard deviations.

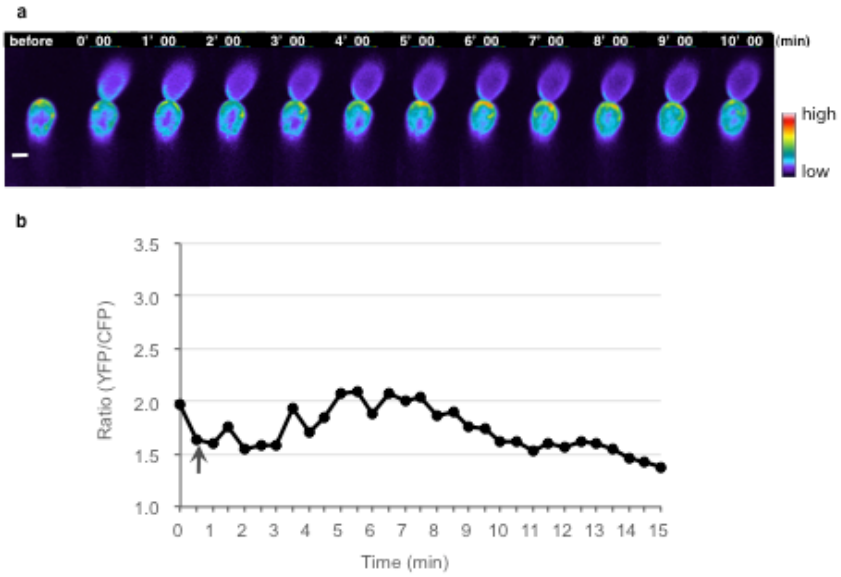

Supplementary Figure 10 | Dynamics of $[Ca^{2+}]_{cyt}$ in YC3.60$_{pm}$–expressing papilla cells treated with 50 mM AP-5 followed by self-pollination. (a) Typical YFP/CFP ratio images of a single AP-5–pretreated S_b-SRK–expressing papilla cell before and after pollination with a self (S_b-SP11/SCR–expressing) pollen grain. **(b)** Typical time-course ratio change in the tip region below the pollen attachment site after the self-pollination. The arrow indicates the time when pollen was attached.

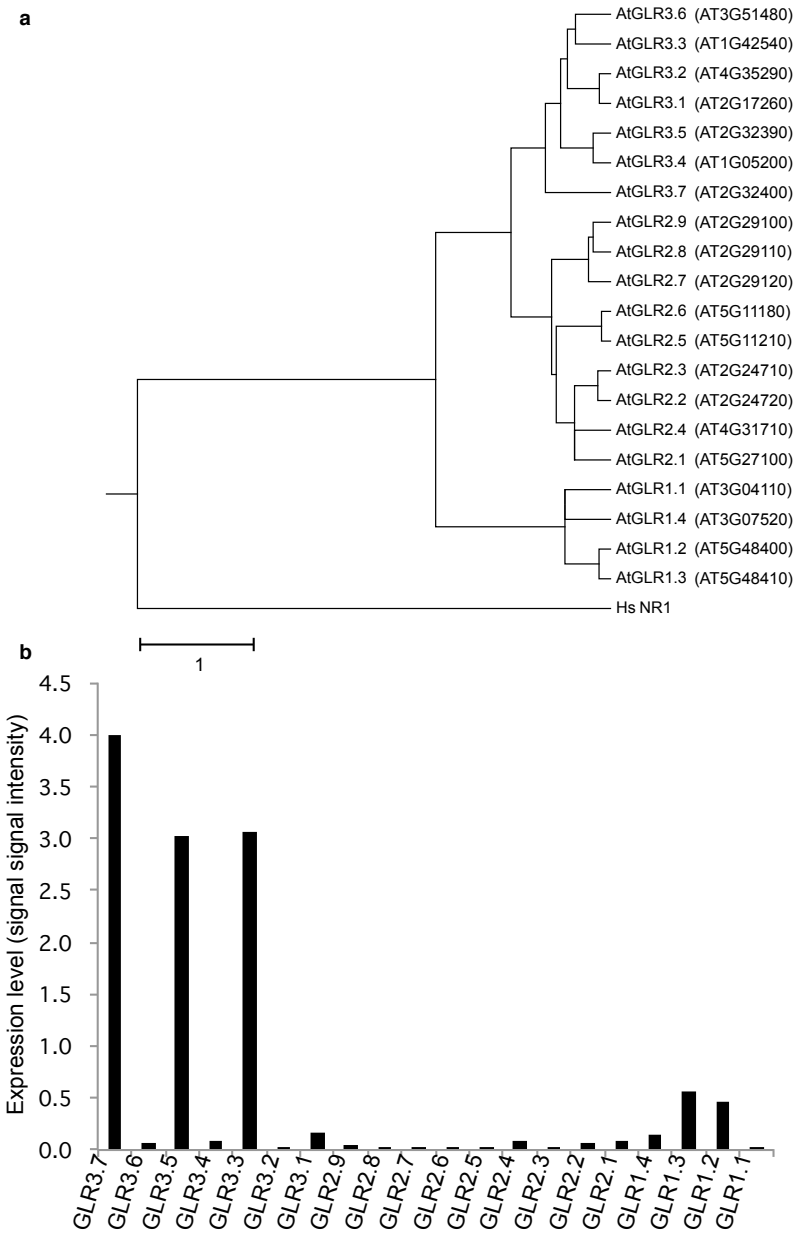

Supplementary Figure 11 | Glutamate receptor-like channel genes in *A. thaliana*. **(a)** Phylogenetic tree of the *GLR* genes predicted in the *A. thaliana* genome. Gene nomenclatures are in line with ref. 54 **(b)** *GLR* gene expression in laser-microdissected papilla cells studied by microarray analysis. Microarray data was deposited to Gene Expression Omnibus at National Center for Biotechnology Information under entry number GSE68205.

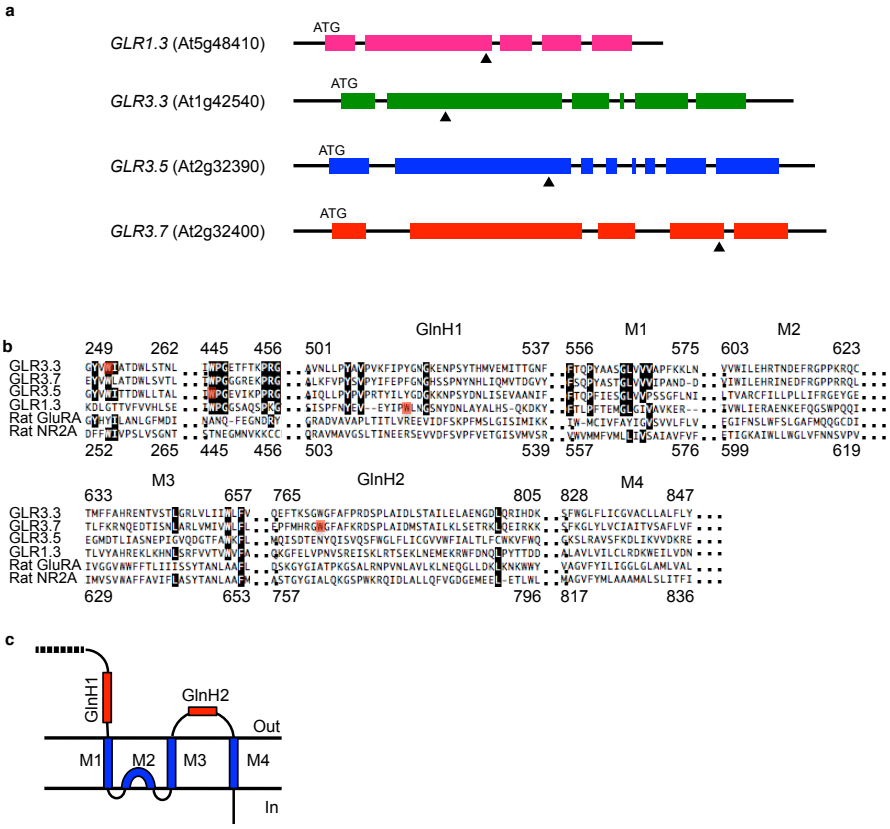

Supplementary Figure 12 | Nonsense mutation in the *glr* mutants. (a) Approximate location of the nonsense mutations on *GLR* gene structures. **(b)** Amino acid sequence alignment of the GLR proteins. Locations where the stop codons are introduced are highlighted in red. GlnH1 and GlnH2 indicate the ligand binding domain of the glutamate receptors in mammals. M1 to M4 indicate the transmembrane domain. **(c)** Schematic structural diagram of the typical glutamate receptor in mammals.

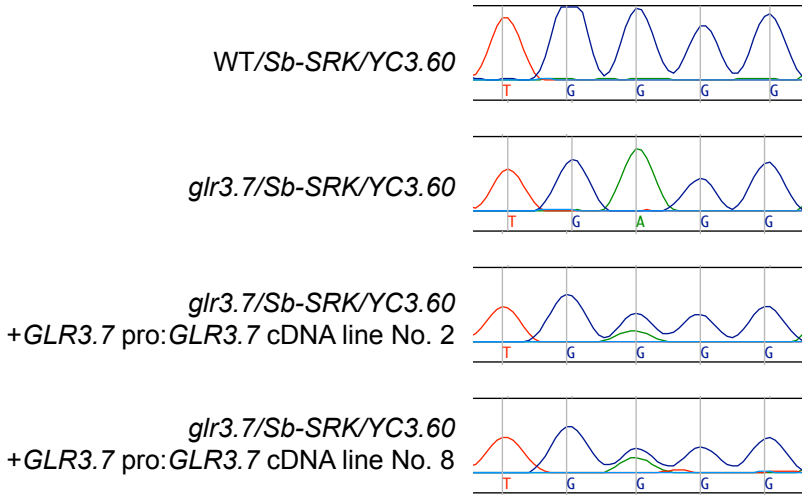

Supplementary Figure 13 | *GLR3.7* cDNA sequence in the *glr3.7* mutant. *GLR3.7* cDNA fragments amplified by RT-PCR were directly sequenced. mRNA expression of the WT cDNA fragment in the gene complemented lines were confirmed.

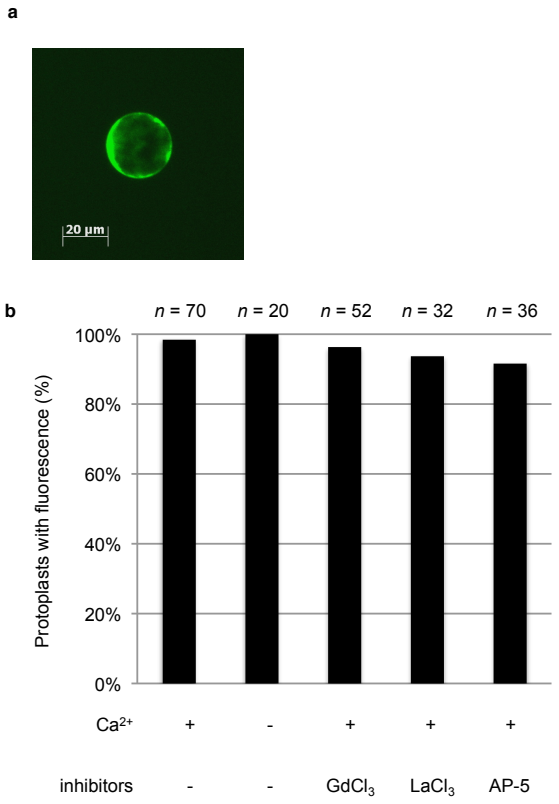

Supplementary Figure 14 | Protoplast viability test after SP11 addition. (a) Typical epifluorescent microscopy image of the protoplast after FDA treatment. **(b)** Percentage of protoplasts with fluorescence under different experimental conditions.

Caption for Supplemental Movie 1. Calcium imaging in a papilla cell during self-pollination. YFP/CFP ratio change in a single S_b-SRK–expressing papilla cell before and after pollination with self (S_b-SP11/SCR–expressing) pollen. Imaging was performed using a confocal laser-scanning microscope equipped with a 440-nm laser (LSM710; Carl Zeiss, Germany). Imaging of the YC3.60 emission ratio was performed using two emission ranges (465-495 for CFP and 515-555 for YFP) using a Zeiss 20×/0.8 fluorescence objective lens. Exposure time was 1 sec, and images were collected every 30 sec.

Caption for Supplemental Movie 2. Calcium imaging in a papilla cell during cross-pollination. YFP/CFP ratio change in a single S_b-SRK–expressing papilla cell before and after pollination with cross (WT) pollen. Imaging was performed using a confocal laser-scanning microscope equipped with a 440-nm laser (LSM710; Carl Zeiss, Germany). Imaging of the YC3.60 emission ratio was performed using two emission ranges (465-495 for CFP and 515-555 for YFP) using a Zeiss 20×/0.8 fluorescence objective lens. Exposure time was 1 sec, and images were collected every 30 sec.

References list

50. Shiba, H. *et al*. A pollen coat protein, SP11/SCR, determines the pollen *S*-specificity in the self-incompatibility of *Brassica* species. *Plant Physiol.* **125,** 2095-2103 (2001).
51. Suzuki, G. *et al*. Genomic organization of the *S* locus: identification and characterization of genes in *SLG/SRK* region of S_9 haplotype of *Brassica campestris* (syn. *rapa*). *Genetics* **153,** 391-400 (1999).
52. Jones, J. D. *et al*. Effective vectors for transformation, expression of heterologous genes, and assaying transposon excision in transgenic plants. *Transgenic Res.* **1,** 285-297 (1992).
53. Lai, K.-S., Kaothien-Nakayama, P., Iwano, M. & Takayama, S. A TILLING resource for functional genomics in Arabidopsis thaliana accession C24. *Genes Genet. Syst.* **87**, 291–297 (2012).
54. Davenport, R. Glutamate receptors in plants. *Ann. Bot.* **90**, 549-557 (2002).